

# Violation of detailed balance for charge-transfer statistics in Coulomb-blockade systems

Philipp Stegmann<sup>\*,1</sup> and Jürgen König<sup>1</sup>

<sup>1</sup>Theoretische Physik, Universität Duisburg-Essen and CENIDE, 47048 Duisburg, Germany

**Key words:** quantum dots, single-electron tunneling, full counting statistics, detailed balance

\* Corresponding author: e-mail philipp.stegmann@uni-due.de, Phone: +49-203-379-3323, Fax: +49-203-379-3665

We discuss the possibility to generate in Coulomb-blockade systems steady states that violate detailed balance. This includes both voltage biased and non-biased scenarios. The violation of detailed balance yields that the charge-transfer statistics for electrons tunneling into

an island experiencing strong Coulomb interaction is different from the statistics for tunneling out. This can be experimentally tested by time-resolved measurement of the island's charge state. We demonstrate this claim for two model systems.

Copyright line will be provided by the publisher

**1 Introduction** Tunneling of electrons into and out of Coulomb-blockade devices such as semiconductor quantum dots or metallic single-electron boxes is a stochastic process. The dynamics of the system is governed by the tunneling rates for the transition between different states of the confined region (quantum dot or single-electron box), in the following referred to as the island. The island state is characterized by its total charge but may also possess other degrees of freedom such as spin. The tunneling rates enter a rate equation that can be used to calculate the time average of quantities such as the island charge, the current through the island, or the current noise.

However, recent progress in nanotechnology has made it possible to monitor tunneling into and out of individual electrons in a time resolved manner. For this, the island has been electrostatically coupled to a sensitive electrometer. In the case of quantum dots, the current through an electrostatically-coupled quantum point contact indicates the island's charge state [1,2,3,4,5,6,7,8,9]. Similarly, the charge state of a metallic single-electron box can be detected via the current through an electrostatically-coupled single electron transistor [10,11,12,13,14]. Also other, e.g., optical [15] or interferometric [16], detection schemes are conceivable. In all cases, the measured time trace of the detector allows for studying the full counting statistics of the charge transfer between island and leads. Counting statistics has recently been utilized to

feedback-control quantum transport [17,18,19] or to study non-Markovian [20,21,22] and frequency-dependent [23,24] processes. Moreover, the impact of ferromagnetic leads [25], electron-phonon interactions [26,27], and the influence of Andreev reflections [28,29,30,31] have been investigated.

Throughout this paper, we only consider steady-state situations, i.e., transient behavior after switching on the device is excluded and counting in the detector starts only after device plus detector have reached their steady state. But we allow for both voltage biased and non-biased scenarios. In the latter case, only one lead is coupled to the island, in the former case, a bias voltage is applied to two leads that drive a current through the island. It is the goal of this paper to show that, in both cases it is possible to generate steady states that violate detailed balance. We illustrate for two specific model systems how the violation of detailed balance is detectable in the tunneling statistics. The issue of detailed-balance violation has recently attracted interest in the statistical-mechanics community [32,33]. Stationary states that violate detailed balance are not fully characterized by the probability distribution alone since closed-loop probability currents occur. This has important implications for computer simulations of stochastic systems. Furthermore, the connection between closed-loop probability currents and entropy production has been investigated.

Copyright line will be provided by the publisher

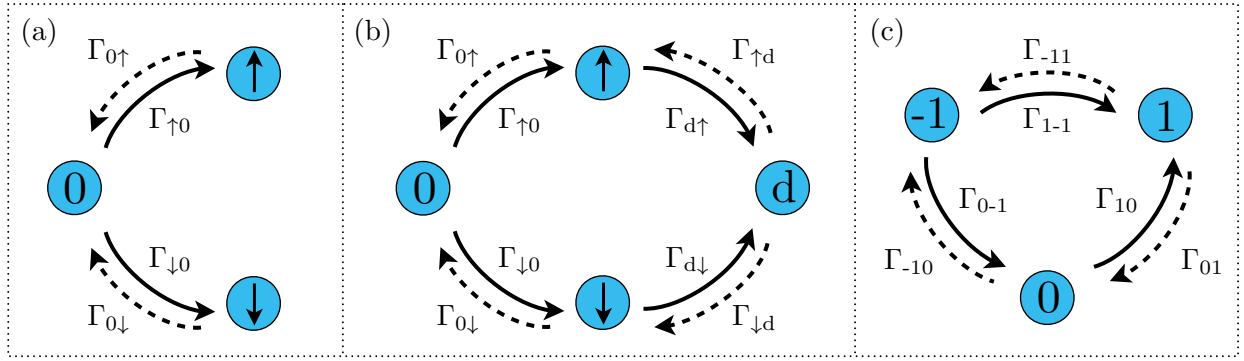


**Figure 1** Three examples of a stochastic model realized in Coulomb-blockade systems. Solid (dashed) lines indicate transitions that are counted for the statistics of tunneling in (out). A violation of detailed balance, indicated by different counting statistics for tunneling in and tunneling out, is possible for model (b) and (c) but not for (a).

**2 Stochastic Systems** A stochastic system is described by the rate equation

$$\dot{p}_\chi = \sum_{\chi' \neq \chi} (\Gamma_{\chi\chi'} p_{\chi'} - \Gamma_{\chi'\chi} p_\chi), \quad (1)$$

where  $p_\chi$  is the probability of the system to be in state  $\chi$  and  $\Gamma_{\chi'\chi}$  is the transition rate from state  $\chi$  to  $\chi'$ . In the steady-state limit, the probability distribution  $\{p_\chi\}$  is time independent, i.e., the time derivative  $\dot{p}_\chi$  vanishes and the sum on the right-hand side of Eq. (1) is zero.

**2.1 Detailed Balance** The stationary state is said to obey detailed balance if not only the *sum* but *each summand* on the right-hand side of Eq. (1) vanishes,

$$\Gamma_{\chi\chi'} p_{\chi'} = \Gamma_{\chi'\chi} p_\chi, \quad (2)$$

for each pair  $\chi, \chi'$  [32,33]. The combination  $\Gamma_{\chi'\chi} p_\chi$  can be interpreted as the probability current for the system to flow from state  $\chi$  to  $\chi'$ . Detailed balance, then, means that the probability current from  $\chi$  to  $\chi'$  minus the one from  $\chi'$  to  $\chi$  is zero, i.e., the net probability current is zero  $I_{\chi'\chi} = \Gamma_{\chi'\chi} p_\chi - \Gamma_{\chi\chi'} p_{\chi'} = 0$  [34].

To illustrate its implications, let us consider the following three stochastic systems that will be relevant for the discussion in the second part of the paper. The first one, sketched in Fig. 1a, consists of three states labeled by  $\chi = 0, \uparrow, \downarrow$ , and transitions are allowed between 0 and  $\uparrow$  as well as between 0 and  $\downarrow$  but not directly between  $\uparrow$  and  $\downarrow$ . In this case, the stationary state must obey detailed balance, as otherwise the net probability current  $I_{\uparrow 0}$  or  $I_{\downarrow 0}$  would be non-zero, which is incompatible with the steady-state condition.

Next, we extend the model by adding a fourth state  $d$  with transition rates from and to the states  $\uparrow$  and  $\downarrow$ , see Fig. 1b. Depending on the values of the rates, this system can accommodate steady states that do not obey detailed balance. In such a state, there is a finite net probability current flowing around the loop  $0 \rightarrow \uparrow \rightarrow d \rightarrow \downarrow \rightarrow 0$  (or in the opposite direction  $0 \rightarrow \downarrow \rightarrow d \rightarrow \uparrow \rightarrow 0$ ).

Detailed-balance violating steady states are already possible for stochastic systems consisting of three states, but only if direct transitions between all the states  $-1, 0, 1$  are allowed, see Fig. 1c, and the tunneling rates are chosen properly.

**2.2 Full Counting Statistics** In Coulomb-blockade devices, steady states that violate detailed balance can be detected by analyzing the charge-transfer statistics. The latter is accessible by a time-resolved measurement of the island's charge state. Let us assume that, in the models sketched in Figs. 1a and 1b, the detector can distinguish between a quantum dot being empty, 0, being singly occupied with  $\uparrow$  or  $\downarrow$  (without being sensitive to the spin degree of freedom), and being doubly occupied,  $d$ . In the model sketched in Fig. 1c, we assume the detector to distinguish between three different charge states  $-1, 0$ , and  $1$  (relative to some reference charge).

In the time trace of the detector current one can identify all tunneling events in which an electron has tunneled *into* the island (solid lines in Fig. 1). By slicing the full time trace into intervals of length  $t$  each, one can obtain the distribution of the probabilities  $P_N^{\text{in}}(t)$  that  $N$  (with  $N \geq 0$ ) electrons have tunneled into the island within a time span of length  $t$ . Alternatively, one may decide to count only electrons tunneling *out* (dashed lines in Fig. 1) to obtain the distribution  $P_N^{\text{out}}(t)$ . Detailed balance implies that the two distributions for tunneling in and tunneling out are identical, since then the probability to find a given sequence of island states,  $\chi_1 \rightarrow \chi_2 \rightarrow \dots \rightarrow \chi_k$ , is the same as finding the opposite sequence,  $\chi_k \rightarrow \dots \rightarrow \chi_2 \rightarrow \chi_1$ . Therefore, a difference between  $P_N^{\text{in}}(t)$  and  $P_N^{\text{out}}(t)$  signals the violation of detailed balance. However, the reverse statement is not necessarily true: a violation of detailed balance may or may not yield a difference between  $P_N^{\text{in}}(t)$  and  $P_N^{\text{out}}(t)$ , depending on which transitions are counted.

A convenient way to quantify any full counting statistics  $P_N(t)$  is to use moments or cumulants. Since, in our case, the stochastic variable  $N$  is an integer

rather than a continuous variable, it is advantageous to employ so-called *factorial* moments, i.e., moments  $\langle N^{(m)} \rangle(t) := \sum_N N^{(m)} P_N(t)$  of the factorial power  $N^{(m)} := N(N-1)\dots(N-m+1)$  rather than the ordinary power  $N^m$  used for ordinary moments. Factorial moments are derived from the generating function

$$\mathcal{M}_F(z, t) := \sum_N (z+1)^N P_N(t), \quad (3)$$

via the derivatives  $\langle N^{(m)} \rangle(t) = \partial_z^m \mathcal{M}_F(z, t)|_{z=0}$  taken at  $z = 0$ . The corresponding factorial cumulants  $C_{F,m}(t) := \langle\langle N^{(m)} \rangle\rangle(t)$  are obtained from

$$C_{F,m}(t) := \frac{\partial^m}{\partial z^m} \ln \mathcal{M}_F(z, t) \Big|_{z=0}. \quad (4)$$

In the context of single-electron tunneling, the use of factorial rather than ordinary cumulants has been suggested [35, 36] as a convenient tool to identify interactions in the system. Furthermore, factorial and generalized factorial cumulants [37] have been analyzed in the short-time limit to detect the presence of fundamental tunneling processes (such as Andreev tunneling) of two electrons simultaneously [38]. Here, we are going to use factorial cumulants to probe the violation of detailed balance by comparing  $C_{F,m}^{\text{in}}(t)$  with  $C_{F,m}^{\text{out}}(t)$ .

To evaluate the generating function for a given stochastic system, we follow along the lines described in Ref. [37]. First, we construct a matrix  $\mathbf{W}_z^{\text{in}}$  in which the matrix element  $(\mathbf{W}_z^{\text{in}})_{\chi'\chi}$  is associated with the transition from state  $\chi$  to state  $\chi'$ . The matrix element is given by the transition rate  $\Gamma_{\chi'\chi}$  times  $z^k$  where  $k$  is number of electrons having entered the island due to the transition. For example, the stochastic model depicted in Fig. 1b yields

$$\mathbf{W}_z^{\text{in}} = \begin{pmatrix} -\Gamma_{\uparrow 0} - \Gamma_{\downarrow 0} & \Gamma_{0\uparrow} & \Gamma_{0\downarrow} & 0 \\ z\Gamma_{\uparrow 0} & -\Gamma_{0\uparrow} - \Gamma_{d\uparrow} & 0 & \Gamma_{\uparrow d} \\ z\Gamma_{\downarrow 0} & 0 & -\Gamma_{0\downarrow} - \Gamma_{d\downarrow} & \Gamma_{\downarrow d} \\ 0 & z\Gamma_{d\uparrow} & z\Gamma_{d\downarrow} & -\Gamma_{\uparrow d} - \Gamma_{\downarrow d} \end{pmatrix}, \quad (5)$$

where rows and columns are arranged to correspond to the states  $0, \uparrow, \downarrow, d$ . In the given example, no term with  $z^2$  appears since [in contrast to the stochastic model shown in Fig. 1c] there is no transition for which the transfer of two electrons is counted. As shown in Ref. [37], the generating function yielding  $C_{F,m}^{\text{in}}$  via Eq. (4) can, then, be expressed as

$$\mathcal{M}_F^{\text{in}}(z, t) = \mathbf{e}^T \cdot \exp(\mathbf{W}_{z+1}^{\text{in}} t) \mathbf{P}_{\text{stat}}, \quad (6)$$

with the vector  $\mathbf{e}^T = (1, 1, \dots, 1)$ . The stationary probability distribution is given by  $\mathbf{W}_1^{\text{in}} \mathbf{P}_{\text{stat}} = 0$  and  $\mathbf{e}^T \cdot \mathbf{P}_{\text{stat}} = 1$ .

For the generating function  $\mathcal{M}_F^{\text{out}}(z, t)$  of  $C_{F,m}^{\text{out}}$ , the matrix  $\mathbf{W}_z^{\text{in}}$  must be replaced by  $\mathbf{W}_z^{\text{out}}$ . Its matrix elements

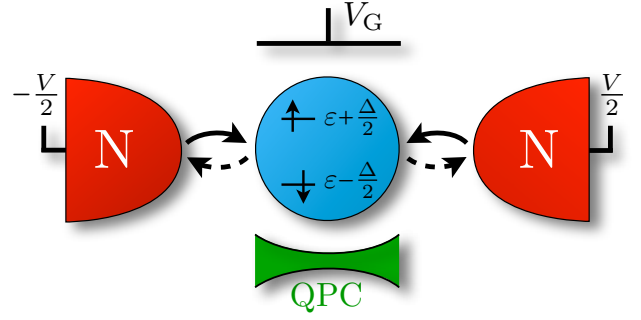


**Figure 2** A single-level quantum dot (blue) subjected to a Zeeman field is tunnel coupled to two metallic leads (red). A bias voltage  $V$  is applied between the leads and the gate voltage  $V_G$  tunes the level position  $\varepsilon$ . The current through a quantum point contact (green) monitors the dot charge as function of time.

are constructed in an identical way as described above, except that  $k$  is the number of electrons having left the island due to the transition. For example, the matrix  $\mathbf{W}_z^{\text{out}}$  of the stochastic model depicted in Fig. 1b is obtained from Eq. (5) if the factors  $z$  are removed from the lower-left off-diagonal matrix elements and put, instead, to the upper-right terms.

**3 Single-level quantum dot with Zeeman field** As a first example, we consider a single-level quantum dot subject to a magnetic field and weakly tunnel coupled to two leads  $r = L, R$  with tunnel-coupling strength  $\Gamma_r$ , see Fig. 2. The Zeeman field  $\Delta$  splits the orbital level  $\varepsilon$  into  $\varepsilon_{\uparrow} = \varepsilon + \Delta/2$  and  $\varepsilon_{\downarrow} = \varepsilon - \Delta/2$  for spin  $\sigma = \uparrow, \downarrow$ . The charging energy for double occupancy is denoted by  $U$ . A bias voltage  $V$  is symmetrically applied to the two leads, described by the electrochemical potentials  $\mu_L = eV/2$  and  $\mu_R = -eV/2$  for the left and right lead, respectively. Fermi's golden rule yields tunneling rates

$$\Gamma_{\sigma 0} = \sum_{r=L,R} \Gamma_r f_r(\varepsilon_{\sigma}), \quad (7)$$

$$\Gamma_{0\sigma} = \sum_{r=L,R} \Gamma_r [1 - f_r(\varepsilon_{\sigma})], \quad (8)$$

$$\Gamma_{d\sigma} = \sum_{r=L,R} \Gamma_r f_r(\varepsilon_{\bar{\sigma}} + U), \quad (9)$$

$$\Gamma_{\sigma d} = \sum_{r=L,R} \Gamma_r [1 - f_r(\varepsilon_{\bar{\sigma}} + U)]. \quad (10)$$

Here, we made use of the Fermi function  $f_r(x) = 1/\{\exp[(x - \mu_r)/k_B T] + 1\}$  and  $\bar{\sigma}$  is the spin opposite to  $\sigma$ .

In Fig. 3a, we show the current as a function of level energy  $\varepsilon$  and bias voltage  $V$ . In the white region, the dot remains in its ground state due to Coulomb blockade. In the colored regions, transitions to other states become possible.

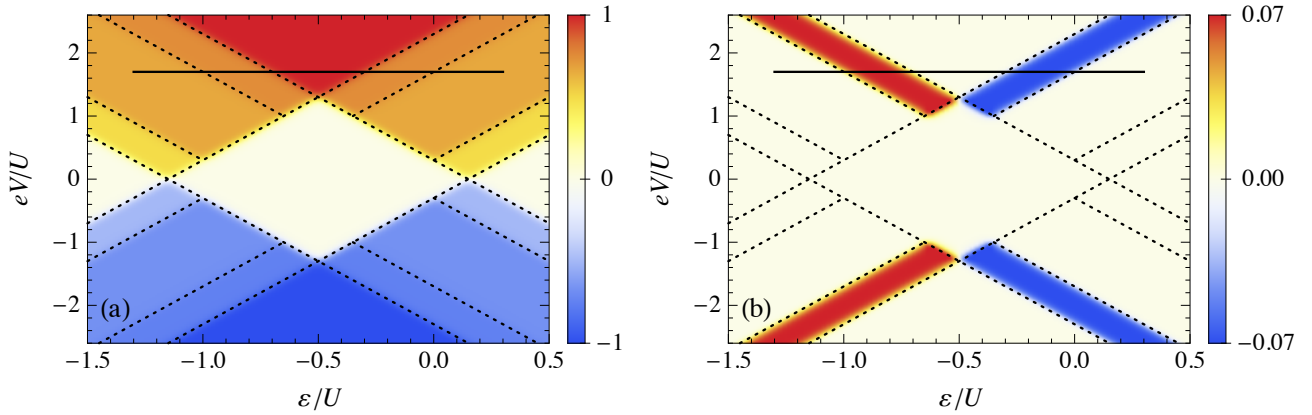


**Figure 3** (a) Current in units of  $e\Gamma_L$  through the quantum-dot system depicted in Fig. 2. (b) The difference  $C_{F,2}^{\text{in}} - C_{F,2}^{\text{out}}$  of the second factorial cumulant as function of the level energy  $\varepsilon$  and bias voltage  $V$ . The parameters are  $\Delta = 0.3U$ ,  $k_B T = 0.02U$ ,  $\Gamma_L = \Gamma_R$ , and  $t = 2/\Gamma_L$ . The dotted lines mark positions of the resonances of the quantum-dot excitation energies with the the Fermi level of the source or drain electrode. A nonvanishing value of  $C_{F,2}^{\text{in}} - C_{F,2}^{\text{out}}$  in (b) indicates the violation of detailed balance.

ble. In most areas of the parameter space, detailed balance holds. However, as depicted in Fig. 3b, there are also areas where detailed balance is violated, which is indicated by a nonvanishing difference  $C_{F,2}^{\text{in}} - C_{F,2}^{\text{out}}$ .

In Fig. 4, we depict the factorial cumulants  $C_{F,m}^{\text{in}}(t)$  (solid lines) and  $C_{F,m}^{\text{out}}(t)$  (dashed lines) as a function of the orbital level energy  $\varepsilon$  for a given bias voltage indicated by the black line in Fig. 3. For  $0 < \varepsilon/U$ , double occupation of the quantum dot is suppressed such that the device is a realization of the stochastic model shown in Fig. 1a, for which detailed balance is expected to be obeyed. Thus, the

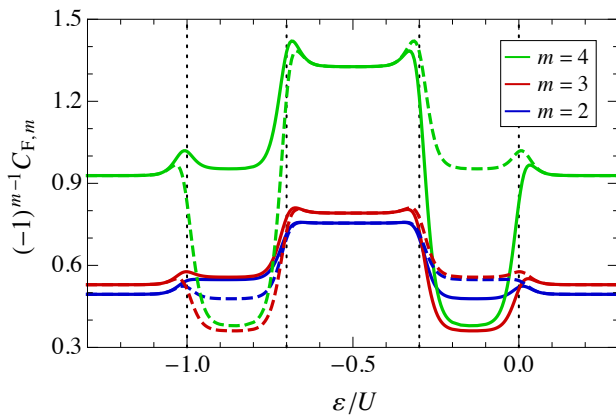


**Figure 4** Factorial cumulants of tunneling in  $C_{F,m}^{\text{in}}$  (solid lines) and tunneling out events  $C_{F,m}^{\text{out}}$  (dashed lines). The parameters are the same as in Fig. 3 with  $eV = 1.7U$ . The dotted vertical lines indicate the positions of the resonances of the quantum-dot excitation energies with the the Fermi level of the source or drain electrode.

factorial cumulants are the same for the tunneling-in and tunneling-out statistics.

This is qualitatively different for  $-0.3 < \varepsilon/U < 0$ . All transitions depicted in Fig. 1b are possible, except the transition from  $\downarrow$  to  $d$ , i.e.,  $\Gamma_{d\downarrow} = 0$ . Since both the probabilities  $p_\downarrow$  and  $p_d$  are finite, detailed balance Eq. (2) is violated. We find a clear difference between the factorial cumulants of the tunneling-in and the tunneling-out statistics for all cumulants of order  $m \geq 2$ , see Fig. 4. Of course, the first cumulants of tunneling in and tunneling out are identical, which is a consequence of the system being in a steady state (note that the first cumulant is equal to the mean number  $\langle N \rangle$ ).

For  $-0.7 < \varepsilon/U < -0.3$ , also the transition  $\downarrow$  to  $d$  becomes possible and detailed balance is reestablish.

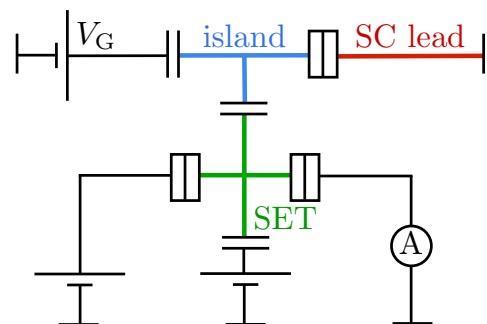


**Figure 5** A normal-state metallic island (blue) tunnel coupled to one superconducting lead (red). Via the gate voltage  $V_G$ , the gate charge  $n_G$  of the island can be tuned. The current through a single-electron transistor (green) monitors the island charge state as function of time.

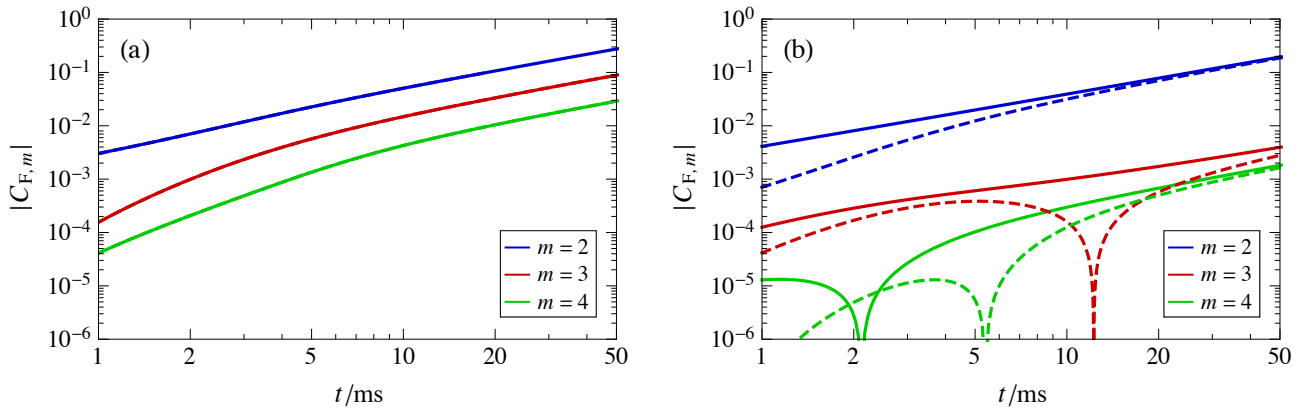


**Figure 6** Factorial cumulants for the single-electron-box system depicted in Fig. 5. Solid lines show  $C_{F,m}^{\text{in}}$  of tunneling-in events and dashed lines represent  $C_{F,m}^{\text{out}}$  of tunneling-out events. In (a), the gate charge is chosen  $n_G = 0$  such that the charge states  $-1$  and  $1$  are degenerate. Detailed balance is fulfilled and thus solid and dashed lines coincide,  $C_{F,m}^{\text{in}} = C_{F,m}^{\text{out}}$ . In (b), we chose  $n_G = 0.12$ . Violation of detailed balance is indicated by  $C_{F,m}^{\text{in}} \neq C_{F,m}^{\text{out}}$ .

Factorial cumulants are the same for the tunneling-in and tunneling-out statistics. For even smaller level positions  $\varepsilon$ , the upper discussion can be repeated due to particle hole symmetry.

We remark that in order to violate detailed balance, it was crucial to break the symmetry between spin  $\uparrow$  and  $\downarrow$  as well as the symmetry between  $0$  and  $d$ . Without a Zeeman field  $\Delta = 0$  or Coulomb interaction  $U = 0$ , detailed balance is recovered. Only with a finite Zeeman field and Coulomb interaction, there are the regions in parameter space, as depicted in Fig. 3b, where detailed balance is violated.

Furthermore, we realize that for the proposed quantum-dot system, a finite bias voltage was applied to achieve a violation of detailed balance, because, otherwise, we could not overcome the charging energy to occupy three different charge states with a finite probability. There is, however, no fundamental reason to require a bias voltage for breaking detailed balance. In fact, in the next section, we are going to show an example that already works without bias voltage.

#### 4 Single-electron box with superconducting lead

Next, we consider a device, see Fig. 5 that has been experimentally realized in Refs. [39,40,41]. A normal metal single-electron box is weakly tunnel coupled to a superconductor and electrostatically coupled to a normal-conducting single-electron transistor that is sensitive to the charge state of the box. At low temperature, only three charge states  $-1, 0, 1$ , relative to some reference charge, play a role. Quasiparticle tunneling induces transitions that change the island's charge by  $\pm 1$ . In addition, there is Andreev tunneling, which directly couples the states  $-1$  and  $1$  and, therefore, changes the island's charge by  $\pm 2$  [as a consequence, counting an Andreev tunneling-in and -out

event contributes with a factor of 2 to  $P_N^{\text{in}}(t)$  and  $P_N^{\text{out}}(t)$ , respectively]. This device is a realization of the stochastic system sketched in Fig. 1c, with

$$\mathbf{W}_z^{\text{in}} = \begin{pmatrix} -\Gamma_{0-1} - \Gamma_{1-1} & \Gamma_{-10} & \Gamma_{-11} \\ z\Gamma_{0-1} & -\Gamma_{-10} - \Gamma_{10} & \Gamma_{01} \\ z^2\Gamma_{1-1} & z\Gamma_{10} & -\Gamma_{-11} - \Gamma_{01} \end{pmatrix}. \quad (11)$$

Again, the matrix  $\mathbf{W}_z^{\text{out}}$  is obtained by removing the factors  $z$  and  $z^2$  from the lower left and adding them to the upper right matrix elements.

The tunneling rates depend on the (normal-state) tunnel resistance, the energies of the different charge states and the coupling to the electromagnetic environment [39, 42]. In order to make close contact to possible experimental realizations, we do not calculate the tunneling rates for some assumed electromagnetic environment, but rather use experimentally measured values taken from Fig. 3b of Ref. [40]. We do this for two different choices of the gate voltage.

First, we consider the symmetric case,  $n_G = 0$ , for which the charge states  $-1$  and  $1$  are energetically degenerate. The transition rates are  $\Gamma_{0-1} = \Gamma_{01} = 960$  Hz,  $\Gamma_{-10} = \Gamma_{10} = 9.4$  Hz, and  $\Gamma_{1-1} = \Gamma_{-11} = 150$  Hz. The symmetry guarantees detailed balance, as demonstrated in Fig. 6a. This contrasts with the asymmetric case, for which we choose  $n_G = 0.12$ . The transition rates are  $\Gamma_{0-1} = 1280$  Hz,  $\Gamma_{01} = 650$  Hz,  $\Gamma_{-10} = 6.5$  Hz,  $\Gamma_{10} = 11.5$  Hz,  $\Gamma_{1-1} = 630$  Hz, and  $\Gamma_{-11} = 10.8$  Hz. In this case, the factorial cumulants of order  $m \geq 2$  for tunneling in and tunneling out differ from each other, see Fig. 6b. The dips shown in Fig. 6b indicate sign changes of  $C_{F,m}^{\text{out}}$  and  $C_{F,m}^{\text{in}}$ . They occur independently of each other. At long times, e.g.  $t = 50$  ms, the signs of  $C_{F,m}^{\text{out}}$  and  $C_{F,m}^{\text{in}}$  coincide.



We emphasize that, for this device, Andreev tunneling is crucial to establish steady states that violate detailed balance. Without this charge-transfer channel, there would be no possibility for a finite net probability current around a closed loop.

**5 Conclusion** Time-resolved measurements of electron tunneling into and out of a quantum dot or a single-electron box in the steady-state limit define a suitable tool to test whether or not detailed balance is fulfilled. To generate a steady state that violates detailed balance, one needs to realize a stochastic model with at least three different states and tunneling rates that allow for a finite net probability current around a closed loop. We have suggested two devices in which such detailed-balance-violating steady states can be established: a spin-split, single-level quantum dot at large bias voltage and a metallic single-electron box coupled to a superconductor. Both suggestions seem experimentally feasible with nowadays technology.

**Acknowledgements** We acknowledge financial support from DFG via KO 1987/5 and SFB 1242.

## References

- [1] S. Gustavsson, R. Leturcq, B. Simović, R. Schleser, T. Ihn, P. Studerus, K. Ensslin, D. C. Driscoll, and A. C. Gossard, Counting Statistics of Single Electron Transport in a Quantum Dot, *Phys. Rev. Lett.* **96**, 076605 (2006).
- [2] T. Fujisawa, T. Hayashi, R. Tomita, and Y. Hirayama, Bidirectional Counting of Single Electrons, *Science* **312**, 1634 (2006).
- [3] S. Gustavsson, R. Leturcq, T. Ihn, K. Ensslin, M. Reinwald, and W. Wegscheider, Measurements of higher-order noise correlations in a quantum dot with a finite bandwidth detector, *Phys. Rev. B* **75**, 075314 (2007).
- [4] C. Fricke, F. Hohls, W. Wegscheider, and R. J. Haug, Bimodal counting statistics in single-electron tunneling through a quantum dot, *Phys. Rev. B* **76**, 155307 (2007).
- [5] C. Flindt, C. Fricke, F. Hohls, T. Novotný, K. Netočný, T. Brandes, and R. J. Haug, Universal oscillations in counting statistics, *PNAS* **106**, 10116 (2009).
- [6] S. Gustavsson, M. Leturcq, R. Studer, I. Shorubalko, T. Ihn, K. Ensslin, D. C. Driscoll, and A. C. Gossard, Electron counting in quantum dots, *Surf. Sci. Rep.* **64**, 191 (2009).
- [7] C. Fricke, F. Hohls, C. Flindt, and R. J. Haug, High cumulants in the counting statistics measured for a quantum dot, *Physica E* **42**, 848 (2010).
- [8] C. Fricke, F. Hohls, N. Sethubalasubramanian, L. Fricke, and R. J. Haug, High-order cumulants in the counting statistics of asymmetric quantum dots, *Appl. Phys. Lett.* **96**, 202103 (2010).
- [9] Y. Komijani, T. Choi, F. Nichele, K. Ensslin, T. Ihn, D. Reuter, and A. D. Wieck, Counting statistics of hole transfer in a *p*-type GaAs quantum dot with dense excitation spectrum, *Phys. Rev. B* **88**, 035417 (2013).
- [10] J. M. Martinis, M. Nahum, and H. D. Jensen, Metrological accuracy of the electron pump, *Phys. Rev. Lett.* **72**, 904 (1994).
- [11] P. D. Dresselhaus, L. Ji, S. Han, J. E. Lukens, and K. K. Likharev, Measurement of single electron lifetimes in a multijunction trap, *Phys. Rev. Lett.* **72**, 3226 (1994).
- [12] S. V. Lotkhov, H. Zangerle, A. B. Zorin, and J. Niemeyer, Storage capabilities of a four-junction single-electron trap with an on-chip resistor, *Appl. Phys. Lett.* **75**, 2665 (1999).
- [13] W. Lu, Z. Ji, L. Pfeiffer, K. W. West, and A. J. Rimberg, Real-time detection of electron tunnelling in a quantum dot, *Nature (London)* **423**, 422 (2003).
- [14] J. Bylander, T. Duty, and P. Delsing, Current measurement by real-time counting of single electrons, *Nature (London)* **434**, 361 (2005).
- [15] A. Kurzman, B. Merkel, P. A. Labud, A. Ludwig, A. D. Wieck, A. Lorke, and M. Geller, Optical blocking of electron tunneling into a single self-assembled quantum dot, *Phys. Rev. Lett.* **117**, 017401 (2016).
- [16] D. Dasenbrook and C. Flindt, Dynamical Scheme for Interferometric Measurements of Full Counting Statistics, *arXiv:1605.01926*.
- [17] C. Pörtl, C. Emary, and T. Brandes, Feedback stabilization of pure states in quantum transport, *Phys. Rev. B* **84**, 085302 (2011).
- [18] S. Daryanoosh, H. M. Wiseman, and T. Brandes, Stochastic feedback control of quantum transport to realize a dynamical ensemble of two nonorthogonal pure states, *Phys. Rev. B* **93**, 085127 (2016).
- [19] T. Wagner, P. Strasberg, J. C. Bayer, E. P. Rugerami-gabo, T. Brandes, and R. J. Haug, Squeezing of shot noise using feedback controlled single-electron tunneling, *arXiv:1602.05466*.
- [20] A. Braggio, J. König, and R. Fazio, Full Counting Statistics in Strongly Interacting Systems: Non-Markovian Effects, *Phys. Rev. Lett.* **96**, 026805 (2006).
- [21] C. Flindt, T. Novotný, A. Braggio, M. Sasseti, and A.-P. Jauho, Counting Statistics of Non-Markovian Quantum Stochastic Processes, *Phys. Rev. Lett.* **100**, 150601 (2008).
- [22] C. Flindt, T. Novotný, A. Braggio, and A.-P. Jauho, Counting statistics of transport through Coulomb blockade nanostructures: High-order cumulants and non-Markovian effects, *Phys. Rev. B* **82**, 155407 (2010).
- [23] C. Emary, D. Marcos, R. Aguado, and T. Brandes, Frequency-dependent counting statistics in interacting nanoscale conductors, *Phys. Rev. B* **76**, 161404(R) (2007).
- [24] N. Ubbelohde, C. Fricke, C. Flindt, F. Hohls, and R. J. Haug, Measurement of finite-frequency current statistics in a single-electron transistor, *Nat. Commun.* **3**, 612 (2012).
- [25] S. Lindebaum, D. Urban, and J. König, Spin-induced charge correlations in transport through interacting quantum dots with ferromagnetic leads, *Phys. Rev. B* **79**, 245303 (2009).
- [26] T. L. Schmidt and A. Komnik, Charge transfer statistics of a molecular quantum dot with a vibrational degree of freedom, *Phys. Rev. B* **80**, 041307(R) (2009).
- [27] R. S. Souto, R. Avriker, R. C. Monreal, A. Martín-Rodero, and A. L. Yeyati, Transient dynamics and waiting time distribution of molecular junctions in the polaronic regime, *Phys. Rev. B* **92**, 125435 (2015).
- [28] J. C. Cuevas and W. Belzig, Full Counting Statistics of Multiple Andreev Reflections, *Phys. Rev. Lett.* **91**, 187001 (2003).

- [29] G. Johansson, P. Samuelsson, and Å. Ingeman, Full Counting Statistics of Multiple Andreev Reflection, *Phys. Rev. Lett.* **91**, 187002 (2003).
- [30] S. Pilgram and P. Samuelsson, Noise and Full Counting Statistics of Incoherent Multiple Andreev Reflection, *Phys. Rev. Lett.* **94**, 086806 (2005).
- [31] J. P. Morten, D. Huertas-Hernando, W. Belzig, and A. Brataas, Full counting statistics of crossed Andreev reflection, *Phys. Rev. B* **78**, 224515 (2008).
- [32] R. K. P. Zia and B. Schmittmann, A possible classification of nonequilibrium steady states, *J. Phys. A* **39**, L407 (2006).
- [33] R. K. P. Zia and B. Schmittmann, Probability currents as principal characteristics in the statistical mechanics of nonequilibrium, *J. Stat. Mech.: Theory Exper.* (2007) P07012.
- [34] We remark that, in the literature, the term 'detailed balance' is often defined in a different way: a stochastic system is said to obey detailed balance if the ratio  $\Gamma_{\chi\chi'}/\Gamma_{\chi'\chi}$  of transition rates is given by  $e^{-\beta(E_\chi - E_{\chi'})}$ , where  $E_\chi$  is the energy of state  $\chi$  and  $\beta$  the inverse temperature. It, then, follows that the stationary (equilibrium) probability distribution is described by the Boltzmann factors,  $p_\chi \sim e^{-\beta E_\chi}$  and Eq. (2) holds. However, this alternative definition of detailed balance is not useful for systems for which the equilibrium probability distribution is *not* given by the Boltzmann factors. This is, e.g., the case for the exactly-solvable model of a spinless single-level quantum dot coupled to one lead beyond the weak-coupling limit. There, higher-order tunneling leads to quantum-fluctuation induced broadening such that  $\Gamma_{10}/\Gamma_{01} \neq e^{-\beta(E_1 - E_0)}$  but Eq. (2) still holds. Another example is the single-electron box discussed in Sec. 4.
- [35] D. Kambly, C. Flindt, and M. Büttiker, Factorial cumulants reveal interactions in counting statistics, *Phys. Rev. B* **83**, 075432 (2011).
- [36] D. Kambly and C. Flindt, Time-dependent factorial cumulants in interacting nano-scale systems, *J. Comput. Electron.* **12**, 331 (2013).
- [37] P. Stegmann, B. Sothmann, A. Hucht, and J. König, Detection of interactions via generalized factorial cumulants in systems in and out of equilibrium, *Phys. Rev. B* **92**, 155413 (2015).
- [38] P. Stegmann and J. König, Short-time counting statistics of charge transfer in Coulomb-blockade systems, *Phys. Rev. B* **94**, 125433 (2016).
- [39] O.-P. Saira, M. Möttönen, V. F. Maisi, and J. P. Pekola, Environmentally activated tunneling events in a hybrid single-electron box, *Phys. Rev. B* **82**, 155443 (2010).
- [40] V. F. Maisi, O.-P. Saira, Yu. A. Pashkin, J. S. Tsai, D. V. Averin, and J. P. Pekola, Real-Time Observation of Discrete Andreev Tunneling Events, *Phys. Rev. Lett.* **106**, 217003 (2011).
- [41] V. F. Maisi, D. Kambly, C. Flindt, and J. P. Pekola, Full Counting Statistics of Andreev Tunneling, *Phys. Rev. Lett.* **112**, 036801 (2014).
- [42] J. P. Pekola, V. F. Maisi, S. Kafanov, N. Chekurov, A. Kempinen, Yu. A. Pashkin, O.-P. Saira, M. Möttönen, and J. S. Tsai, Environment-Assisted Tunneling as an Origin of the Dynes Density of States, *Phys. Rev. Lett.* **105**, 026803 (2010).